

**Semi-Automatic Registration Utility for MR Brain Imaging of
Small Animals**

A Thesis

Submitted to the Faculty

of the

WORCESTER POLYTECHNIC INSTITUTE

in partial fulfillment of the requirements for the

Degree of Master of Science

in

MECHANICAL ENGINEERING DEPARTMENT

by

Nov. 2013

APPROVED:

Prof. John M. Sullivan, Thesis Advisor

Prof. Brian J. Sivilonis, Committee Member

Prof. Zhikun Hou, Committee Member

Prof. Raghvendra V. Cowlagi, Graduate Committee Representative

Abstract

The advancements in medical image technologies have allowed more accurate diagnosis and quantitative assessments. Magnetic Resonance Imaging (MRI) is one of the most effective and critical technologies in modern diagnosis. Various researches have been advanced based on MR imaging technique. However, to perform these various topics, preprocessing tasks are required including registration (or alignment), segmentation, and correlation analysis. This thesis aims to develop a semi-automatic registration utility for MR images.

Generally, image registration strategies fall into two categories: intensity-based methods and feature-based methods. This thesis focused on intensity-based since it asks for less user interactions, which is one of the goals of this research. Genetic Algorithm was selected to be the optimization strategy. GA is a very efficient strategy for optimization since it combines both exploration and exploitation well.

The semi-automatic utility was developed for doing MRI registration of small animals. It focuses on 2D rigid body registration since small animals such as rats have similar brain shapes. All sample data was collected from Center for Comparative NeuroImaging (CCNI) a joint venture between WPI and the University of Massachusetts Medical School.

The test results show that this developed utility can perform registration well for MR images of small animals in both intra-subject and inter-subjects.

Acknowledgements

First of all, I would like to express my deepest gratitude to my thesis advisor, Prof. John Sullivan, who provides me with continuous support and help throughout my master program, for his patience, motivation and enthusiasm.

Besides my advisor, I would like to thank the rest of my thesis committee: Prof. Brian Savilonis, Prof. Zhikun Hou and Prof. Cowlagi for their encouragement and insightful comments.

Thanks for the authorization of the Teaching assistantship from Mechanical Engineering Department at WPI.

Thanks for all the suggestion and help from administrative assistants.

Thanks for all friends who have been support me, trust me, and encourage me through the past years.

Thanks for my parents who gave me enormous support and infinite love.

Table of Contents

Abstract	i
Acknowledgements	ii
Table of Contents	iii
List of Figures	v
List of Tables	vi
Chapter 1 Introduction	1
1.1 Motivation	1
1.2 Goals	3
1.3 Methodology	3
1.4 Thesis overviews	4
Chapter 2 Background	5
2.1 Overview of Medical Images	5
2.1.1 X-rays CT	5
2.1.2 Ultrasound	6
2.1.3 Emission-computed tomography	7
2.1.4 Magnetic Resonance Imaging	8
2.1.5 Functional MRI	9
2.2 Image Registration	11
2.2.1 Registration Methods	11
2.2.2 Transformation models	14
2.2.3 Evaluation criteria	16
2.3 Proposed optimization strategies	16
2.3.1 Wavelet-Modulus Maxima method	17
2.3.2 Fast Fourier Transform (FFT) technique	17
2.3.3 Morphological Pyramid Image Registration (MPIR) algorithm	19
2.3.4 Classical genetic algorithm	19
2.3.5 Why GA	21
Chapter 3 Genetic Algorithm for image registration	22
3.1 Genetic Algorithm	22
3.1.1 Selection	23

3.1.2 Crossover	25
3.1.3 Mutation.....	27
3.1.4 Fitness function.....	31
3.2 Implementation	33
3.2.1 Data Sets	33
3.2.2Preprocessing	34
3.2.3 GA registration.....	36
3.3 Sample results	36
Chapter 4 MATLAB GUI.....	40
4.1 Why GUI.....	40
4.2 Screen Sketches	40
Chapter 5 Results	48
5.1 Summary of terms.....	48
5.2 Data sets	49
5.3 Application for functional image registration.....	50
5.4 Application for anatomical image registration	51
5.5 Failures.....	53
Chapter 6 Conclusions	55
References	57

List of Figures

Figure 1: Registration of a 3D brain MR images.....	2
Figure 2: X-ray CT	6
Figure 3: Ultrasound image of a fetus	7
Figure 4: PET scans show different patterns of brain under different mental tasks	8
Figure 5: Magnetic Resonance Imaging of rat brain.	9
Figure 6: An example of functional MRI of a rat brain.....	10
Figure 7: fMRI showing active region of brain	11
Figure 8: Feature based image registration.	12
Figure 9: Basic feature detection.	18
Figure 10: Flow chart of solving problems with Genetic Algorithm.....	20
Figure 11: Illustration of one-point and two-points crossover	26
Figure 12: Uniform crossovers.	26
Figure 13: Illustration of mutation	28
Figure 14:One slice of MRI volumes of rat brain.....	34
Figure 15:One slice of fMRI volumes in a specified time step	34
Figure 16: Region of interested marked within red circle.	35
Figure 17: View of images before and after registration.....	37
Figure 18: View of comparison between before and after registration.	39
Figure 19: User interface for 2D rigid registration with genetic algorithm.....	41
Figure 20: Operation direction.....	41
Figure 21: Selecting registration type.	42
Figure 22: Switching slices by using slider bars.....	44
Figure 23: Cropping reference and subject images.....	45
Figure 24: Display of correlation and growth rate of the changing of correlation	46
Figure 25: an example of low quality images.....	53
Figure 26: example of two images having distinct different.	54

List of Tables

Table 1: Parameters of 2D rigid transformation.	22
Table 2: Image information in sample test.	37
Table 3: Source anatomical images.	49
Table 4: Source functional images.....	50
Table 5: registration results of functional images.....	51
Table 6: registration results of anatomical images.	52

Chapter 1

Introduction

1.1 Motivation

This thesis targets medical image registration or alignment. The highly developed medical image technologies allow more and more accurate diagnosis and quantitative assessment. It is customary for a patient to take multiple medical images through time, in order to monitor the changes inside the body. In traditional therapy, medical images are printed out and viewed side-by-side on light boxes. It's difficult to recognize and quantify small changes using this strategy. Thus, image registration plays a critical role in computer vision and image processing tasks such as motion analysis, video compression, image enhancement and restoration. For example, in a sequential set of MR images of same subject acquired at different times, it is expected that images can be aligned well so that small changes can be noticed. These small changes could be the result of therapeutic treatment or the lack of thereof. Medical image registration is a required component with medical imaging and processing technologies. It refers to the process of aligning images in same or different modalities [1][2], at different times [3][4], and/or different subjects [5][6].

There are multiple stages within a complete medical image analysis, among which image registration is one of the early steps. Frequently, imaging sessions can last several minutes such that motion corrections must be made to negate the effects of breathing, cardiac motions and general patient motion. In these cases, mathematical modeling techniques are required to maintain geometric alignment. These techniques include translation, scaling and rotation of the input images compared to reference or baseline

images. These alignment techniques were used to observe the progression of a brain lesion. [7,8,9]

Registration is defined as a geometrical transformation that aligns one subject image to another object in terms of the corresponding points. Taking brain images for instance, registration can help to align subject brain to reference brain. In Fig. 1, the source image (a) was aligned to the target images (b). Once aligned (c), lesion is readily identified by red arrows.

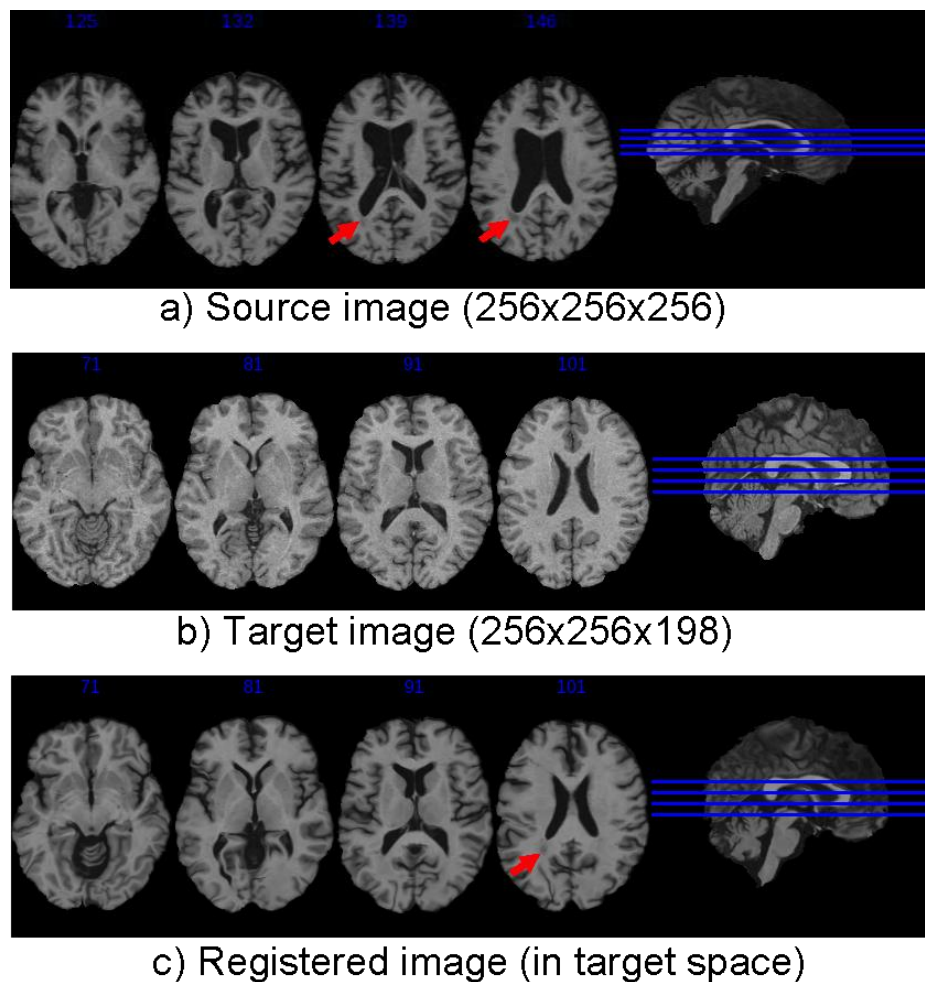


Figure 1: Registration of a 3D brain MR images with lesions onto a healthy brain template [10].

1.2 Goals

Ongoing research endeavors associated with medical image alignments are vast. I have restricted my research to providing translational scientists with an interactive visualization tool to assist their alignment tasks. The underpinning alignment mathematics is based on translation and rotation within a Genetic Algorithm framework.

1.3 Methodology

The translational scientist develops and studies animal models of human diseases and conditions. The use of laboratory rats and mice dominate the animal model populations used in these studies. The size and shape of rat and mice brains are very consistent within each species. Consequently, scaling and non-linear alignment strategies are rarely warranted in these subjects. The major alignment variability is associated with the subject's placement within the imaging system, which can be corrected with translational and rotational alignment techniques. There are two major alignment methodologies. One category is fiducial alignment, which is might be the alignment based on the perimeter outline or a characteristic trait within an image. The other category is intensity-based registration, which involves the pixel-by-pixel gray-scale intensity comparisons amongst image volumes. This thesis concentrated on intensity-based comparisons. It uses a Genetic Algorithm as the optimization strategy. Data sets used in this research are Magnetic Resonance Images of rat brains collected at the Center for Comparative NeuroImaging, a joint venture between WPI and the University Of Massachusetts Medical School. Algorithms are implemented within MATLAB. The interactive user

interface was built using MATLAB GUIDE (Graphic User Interface Development Environment).

1.4 Thesis overviews

This thesis is organized as follows:

Chapter 2 introduces existing modalities of medical image, image registration models and proposed registration strategies.

Chapter 3 describes Genetic Algorithm and implementation of GA.

Chapter 4 introduces user interface created on MATLAB Graphic User Interface development environment including functions and operations.

Chapter 5 presents results, presents numerous results for 2D rigid image registration.

Chapter 6 draws the conclusions and suggests future works in related research.

Chapter 2

Background

2.1 Overview of Medical Images

Medical images are widely used in modern medical research and clinical diagnoses since they can provide clear and non-invasive visualization of internal organs, tissue, etc. These tomographic technologies allows three or four-dimensional representations. Major modalities of medical imaging include projection X-ray computed tomography (CT), ultrasound, magnetic resonance imaging (MRI), etc. [11] In each of these modalities, a set of 2D slices with array of intensity values are collected together to provide a 3D volume. Typical 2D image slices may be captured on film or acquired digitally. In this research, we concerned primarily with digital images as array of intensity values. The various volumes can be acquired from the same subject (intra-patient), or from different subjects (inter-patient).

2.1.1 X-rays CT

X-ray CT is widely used in medical diagnosis by providing a volume of data that can be manipulated to represent a patient's anatomy. Most current X-ray CT scanners generate 3D volume at the rate of one 2D slice at a time, such as Fig.2 [12]. The X-ray image is obtained by placing part of the patient in front of X-ray detector with X-ray pulse. The great majority of CT uses gamma-ray emitter as a source. The detectors record the exiting x-rays. As the x-ray source rotates, detector records at each position (angle) of source in a complete rotation. Then, those data are sent to computer so that to generate a complete

image of the exposure part.

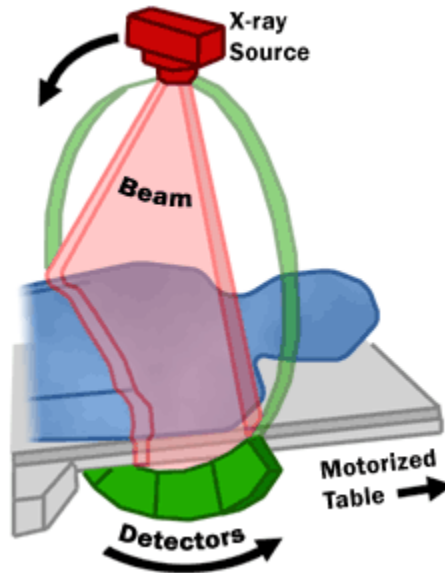


Figure 2: X-ray CT [13].

2.1.2 Ultrasound

Ultrasound images are attractive due to their ability to generate real time inspection. The real time information allows physicians to observe the motion of tissues inside patient's body. In ultrasound imaging, high frequency sound waves, which have been determined to be safe [11], are emitted into patient's body and tissues. The sound waves travel into patients' body and some of them get reflected back by the boundary of tissues (For example, bone and organs). The reflected waves are picked up by the machine. From the measurement of time delay and the intensity of the echoes, an image is reconstructed [13]. Ultrasound imaging technique can be used to capture the soft tissues inside the body in real-time. Since it can show movement of objects, ultrasound can be used in measuring blood flow velocity in a vessel, pregnancy (Fig.3), and other diagnosis.



Figure 3: Ultrasound image of a fetus [14].

2.1.3 Emission-computed tomography

Emission computed tomography (ECT), which is also known as nuclear imaging, is a form of tomography in which the emitted decay products, as positrons or gamma rays are recorded in detectors outside the body. Two main types of ECT are positron emission tomography (PET) and single photon emission computed tomography (SPECT). In both types, doses of tracer containing gamma rays are injected into organs and tissues. Tracers vary depending on the purpose of diagnosis. Images showing chemical changes can be obtained by detecting gamma rays emitted from tracer. PET (Fig.4) scans play an important role in determining cancerous tissue. SPECT scans can provide information including blood flow or chemical reactions in the body.

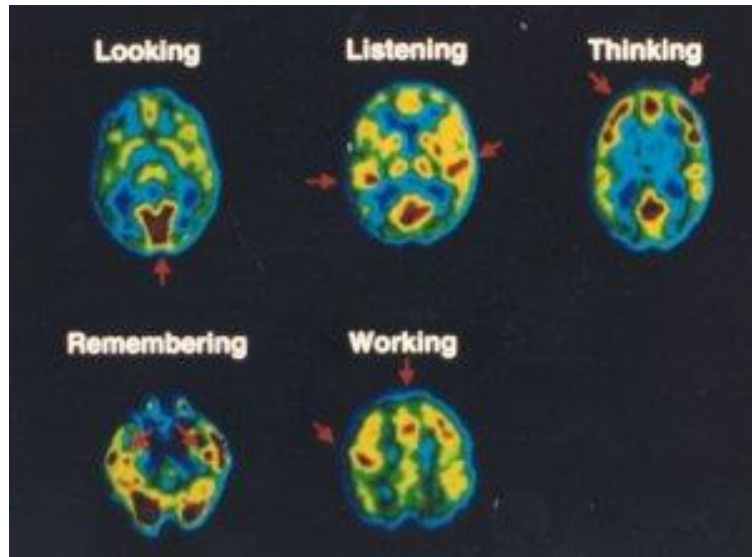


Figure 4: PET scans show different patterns of brain under different mental tasks [15].

2.1.4 Magnetic Resonance Imaging

Magnetic Resonance Imaging (MRI) provides more detailed images of soft tissues amongst the various tomographic imaging modalities. Different from x-ray or CT, radiofrequency pulse used for MRI is found all around us and is harmless to tissue as it passes through. Taking human brain for instance, MRI can provide a sequential scan through axial (Fig. 5 (a)), sagittal (Fig. 5 (b)), and coronal (Fig. 5 (c)) planes [16] and finally a set of slices images. Information between slices can be got by interpolation.

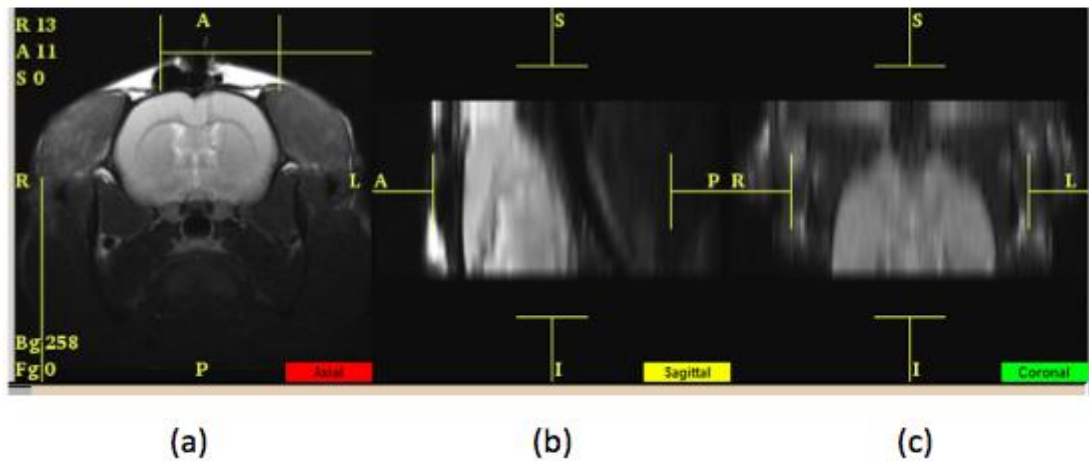


Figure 5: Magnetic Resonance Imaging of rat brain.

Magnetic Resonance imaging (MRI) is a medical imaging technology using radiology to investigate the anatomy and function of the body [17] [11]. A magnetic field sending radio waves through patients' body so that triggers protons to align themselves. When protons are aligned, they absorb energy from radio waves. Once protons are released, they turn to emit energy that would be picked up by receiver. Different organs or tissues have different contrast since they relax at different rates when radiofrequency pulse is turned off. The information is then analyzed and translated into an image.

2.1.5 Functional MRI

Functional MRI is a non-invasive imaging method using MRI to monitor behavioral and/or physical changes to a body region continuously through time. During an fMRI experiment, a series of brain images are taken while the brain is performing a task, for example. Since brain functions can be spatially separated, functional specialization can be detected by fMRI when a specific region of the brain is stimulated. Compared to MRI, fMRI has lower resolution (such as Fig.6), thus taking less time to obtain one slice.

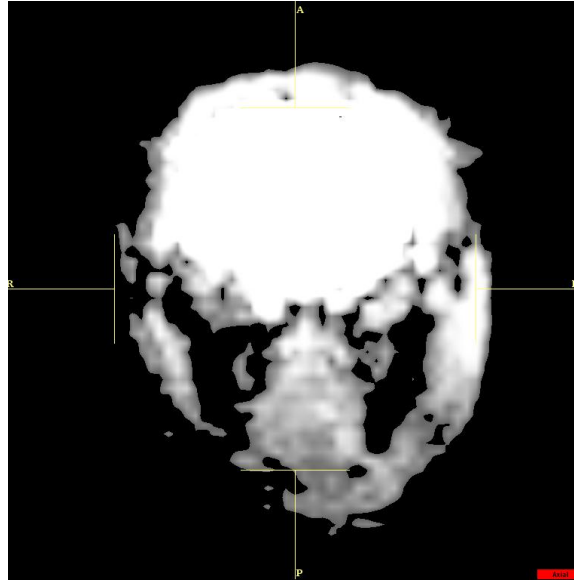


Figure 6: An example of functional MRI of a rat brain.

fMRI technique relies on a fact that cerebral blood and neural activations are coupled. Hence, the level of oxygen in the blood is translated to how active is that portion of the brain. The image shown in Fig. 7 is an example showing an anatomy brain image under a specific mental task. The red and blue regions delineate increased and decreased oxygen changes, respectively. This form of functional imaging is known as BOLD (Blood Oxygen Level Dependent) method [17]. In Fig. 7, the red region has high oxygen level, which means in highly active state, while blue region has relatively low oxygen level which means in less active state. Regions without color are in non-active state.

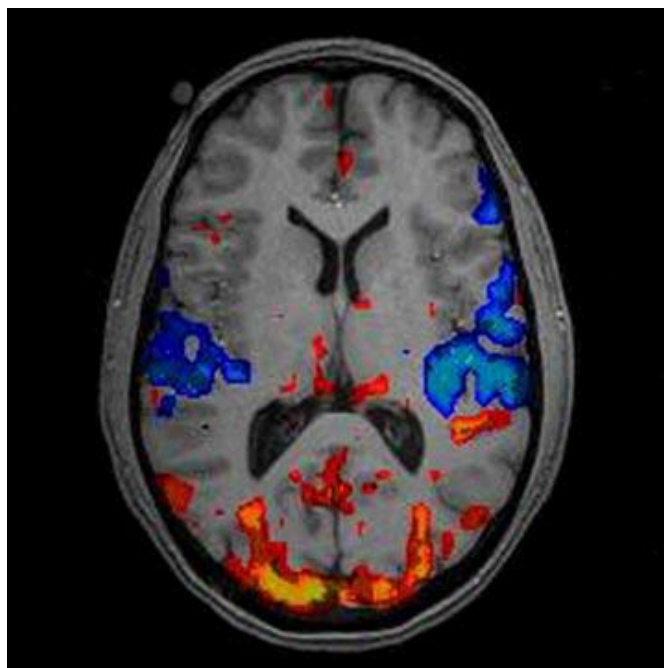


Figure 7: fMRI showing active region of brain [18].

2.2 Image Registration

2.2.1 Registration Methods

Registration (or image alignment) is a fundamental task in image processing that can be performed by either manually, semi-automatic, or fully automatically requiring no user intervention. Manually registration requires an experienced scientist or technician for successful alignments. This methodology takes considerable time and scales linearly with the number of subjects to be aligned. Naturally, there is a need for automatic registration algorithms. Usually, automatic registration theory can be classified into intensity-based and feature-based.

Feature-based registration:

Feature-based or fiducial registration approaches attempt to align standard features that extracted from images. There are two procedures for feature-based registration: feature extraction and feature correspondence [19]. In the former procedure, features, or landmarks, of images can be extracted from special domain or transformed domain. Special domain components include points (such as Fig.8), curves, and surface model [12]. While in transformed domain, images are represented by a set of transform coefficients. By aligning corresponding features in each images volume set, image registration can be done among multiple modalities or images with different gray-levels. However, feature extraction is a very difficult problem independent of the alignment methodology, manual, semi-automatic, or automatic.

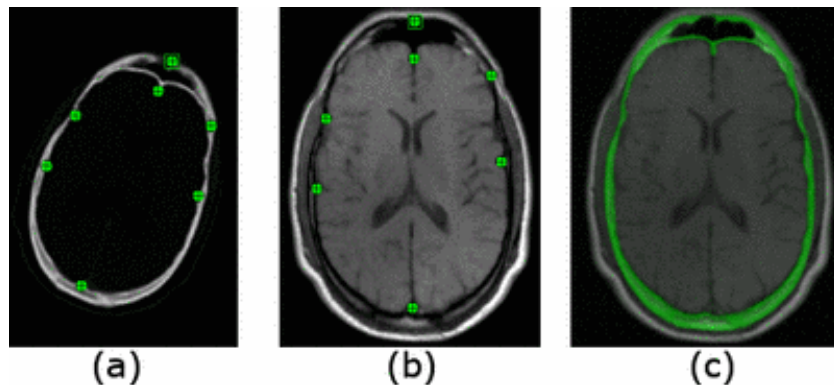


Figure 8: Feature based image registration. Corresponding landmarks were identified in both, the CT image (a) and the MR image (b), (c) Provides both images after registration [20].

Intensity-based registration:

Intensity-based registration is a transformed process based on intensity value differences between volume image sets. The basic principle of intensity-based image registration is to minimize the pixel intensity differences between subject and reference volume sets. By

applying a certain transformation, intensity values of the original pixels are placed at the transformed locations. Then, the calculation of similarity is performed between two images using pixel or voxel values. In practice, many intensity-based registration algorithm only need a subset of the pixels or voxels workspace, which allows the algorithm to run faster. An alignment algorithm usually works more reliably if the measurements between pixels are based on the region of interest (RIO), rather than all pixels. Compared to strategies like feature-based [21], point-based [22] and surface-based [23] registration, a major attraction of intensity-based registration is the reduced user-interaction time. As a result, intensity-based registration is easier to automate. Measurements based on intensity value are widely used in registration problems, including [24], [25]:

1. 2-D or 3-D images rigid-body registration between same subjects that taken at different times with the same modality
2. 2-D or 3-D images rigid-body registration between same subjects that taken at different times with different modalities
3. Non-rigid registration between same subject images that taken at different times
4. 3-D non-rigid inter-subject registration

In this thesis, registration was done based on intensity values since our concentration is 2-D rigid registration all on MR images. A major attraction for intensity-based registration is the reduced user-interaction time requirement compared to feature-based registration. Additionally, it does not require the same level of experience as that required for abstraction of features within images. As a consequence, intensity-based methods are easier for automatic registration.

2.2.2 Transformation models

Transformation matrices are special matrices that can describe 2-D and 3-D transformations. In three dimensions, a rigid body transformation is defined by six parameters. These parameters include three translation (dx, dy, dz) and three rotations about orthogonal axes. Usually 3D linear transformation matrix is applied as:

$$\begin{bmatrix} X' \\ Y' \\ Z' \end{bmatrix} = \begin{bmatrix} a_1 & b_1 & c_1 \\ a_2 & b_2 & c_2 \\ a_3 & b_3 & c_3 \end{bmatrix} \cdot \begin{bmatrix} X \\ Y \\ Z \end{bmatrix} + \begin{bmatrix} d_1 \\ d_2 \\ d_3 \end{bmatrix} \quad (1)$$

$$I' = M \cdot I + d \quad (2)$$

However, another equivalent rotational strategy coupled with scaling on a subject can be expressed in a single matrix as:

$$M = R_X \cdot R_Y \cdot R_Z \cdot S \quad (3)$$

To combine translation, rotation and scale into one matrix that is more convenient for computing, the 3*3 rotation and scale matrix M and 3*1 translation vector d from the original equations yields a 4*4 matrix T . Using this 4*4 homogeneous transformation matrix allows the combination of rotations, translations, and scales. It also can incorporate shears and reflections into a single matrix. Thus, the 4*4 homogenous transformation matrix is used for this work.

The transformation operator performs a geometric transformation that maps each element from input image into new position in an output image. In this process, the dimensionalities of two images are usually but not limited to be the same. The translation

matrix Tr describes the displacement in x, y, and z directions as:

$$Tr = \begin{matrix} \hat{e}_x & 1 & 0 & 0 & Dx & \hat{u}_x \\ \hat{e}_y & 0 & 1 & 0 & Dy & \hat{u}_y \\ \hat{e}_z & 0 & 0 & 1 & Dz & \hat{u}_z \\ \hat{e}_0 & 0 & 0 & 0 & 1 & \hat{u}_0 \end{matrix} \quad (4)$$

Rotation matrix R_x describes the rotation about x-axis as:

$$R_x = \begin{matrix} \hat{e}_x & 1 & 0 & 0 & 0 & \hat{u}_x \\ \hat{e}_y & 0 & \cos a & \sin a & 0 & \hat{u}_y \\ \hat{e}_z & 0 & -\sin a & \cos a & 0 & \hat{u}_z \\ \hat{e}_0 & 0 & 0 & 0 & 1 & \hat{u}_0 \end{matrix} \quad (5)$$

Rotation matrix R_y describes the rotation about y-axis as:

$$R_y = \begin{matrix} \hat{e}_x & \cos b & 0 & -\sin b & 0 & \hat{u}_x \\ \hat{e}_y & 0 & 1 & 0 & 0 & \hat{u}_y \\ \hat{e}_z & \sin b & 0 & \cos b & 0 & \hat{u}_z \\ \hat{e}_0 & 0 & 0 & 0 & 1 & \hat{u}_0 \end{matrix} \quad (6)$$

Rotation matrix R_z describes the rotation about z-axis as:

$$R_z = \begin{matrix} \hat{e}_x & \cos q & \sin q & 0 & 0 & \hat{u}_x \\ \hat{e}_y & -\sin q & \cos q & 0 & 0 & \hat{u}_y \\ \hat{e}_z & 0 & 0 & 1 & 0 & \hat{u}_z \\ \hat{e}_0 & 0 & 0 & 0 & 1 & \hat{u}_0 \end{matrix} \quad (7)$$

For non-rigid body, there are three additional parameters as scaling ratios about the origin in x, y, and z direction:

$$S = \begin{matrix} \hat{e}_x & S_x & 0 & 0 & 0 & \hat{u}_x \\ \hat{e}_y & 0 & S_y & 0 & 0 & \hat{u}_y \\ \hat{e}_z & 0 & 0 & S_z & 0 & \hat{u}_z \\ \hat{e}_0 & 0 & 0 & 0 & 1 & \hat{u}_0 \end{matrix} \quad (8)$$

The overall transformation matrix for affine model is the produce of translation, rotation

and scaling:

$$T = Tr \cdot Rx \cdot Ry \cdot Rz \cdot S \quad (9)$$

While in this thesis, the registration is done on 2-D rigid body, thus the number of parameters was reduced to 3: **dx, dy, and θ** .

2.2.3 Evaluation criteria

Evaluation criteria are set to measure the quality of each potential solution. In order to evaluate each transformation solution, the transformed subject is compared to reference image. Evaluation criteria are detailed introduced in Chapter 3.

2.3 Proposed optimization strategies

Proposed optimization strategies of image registration algorithms such as wavelet transformation method, Fast Fourier Transformation technique, Morphological Pyramid approach and Genetic algorithm are widely used in geometric transformation. Each strategy performs well in accuracy, automated solution, low computational cost and other aspects for some applications. According to B.S. Reddy [26] [27], optimization strategies used in image registration are divided into following classes:

1. Algorithms that directly use the pixel values.
2. Algorithms that operate in the frequency domain
3. Algorithms that use low-level features, and
4. Algorithms that use high-level features.

The four algorithms mentioned previously are illustrated and compared to the classes described by Reddy.

2.3.1 Wavelet-Modulus Maxima method

Wavelet-Modulus Maxima method was proposed by Fonesca [28]. A point is taken from subject image and a sub set of pixels around this point is used for correlation coefficient compared with sub sets from reference image. Two pairs of points having the maximum correlation coefficient are chosen to be feature points. Correlation coefficient is calculated between a sub set of pixels around a point from subject image and all sub sets of pixels around each point from reference image. Those two points having highest correlation are selected as feature point. Then, translation and rotation errors between reference and subject images can be corrected through polynomial transform. A 2D MRI image can be treated as two-dimensional signal, in which case, wavelet transform is done separately [29]. By analyzing phase of wavelet transform, singularities and irregular structures are recognized. After an ideal matching is achieved, all final parameters are applied to the original input image. However, there will be discontinuity existed. So the consistency check is done iteratively till acceptable solution is achieved.

2.3.2 Fast Fourier Transform (FFT) technique

Fourier transform technique can convert time or space domain to frequency domain. FFT is a fast algorithm to perform such transformations. If taking a row or column from a image, the intensity values in space domain can be then present as a wave in frequency domain. However, images are always 2D, so that such two such frequency domain waves are required to represent one image. FFT technique is frequency domain approach by FFT ration instead of any control points [24]. A pattern of small features requires small wavelength, thus larger frequency. Similarly large features are transformed into smaller frequency. High frequencies are always shown as a jump in frequency domain (for

example, Fig. 9).

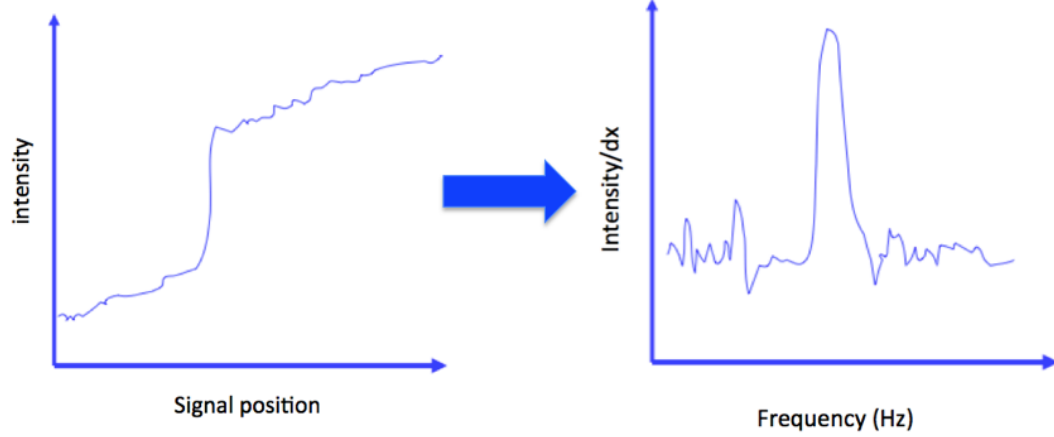


Figure 9: Basic feature detection [30].

FFT method relies on the Fourier shift theorem [31]. If f_1 and f_2 are two images with a shift (x_0, y_0) , then their Fourier transforms are related as [32]:

$$\mathbf{F}_2(\xi, \eta) = \mathbf{e}^{-j2\pi(\xi x_0 + \eta y_0)} \mathbf{F}_1(\xi, \eta) \quad (10)$$

The cross-power spectrum of these two images is defined as:

$$\frac{\mathbf{F}_1(\xi, \eta) * \text{conj}(\mathbf{F}_2(\xi, \eta))}{|\mathbf{F}_1(\xi, \eta) \mathbf{F}_2(\xi, \eta)|} = \mathbf{e}^{-j2\pi(\xi x_0 + \eta y_0)} \quad (11)$$

According to shift theorem, the phase of the cross-power spectrum equal to the phase difference between two images. The inversed Fourier transform is approximately zero everywhere except a small distance around a single point. The location of the single point is (x_0, y_0) . Log-polar coordinate $(\log(r), \theta)$ is then introduced to transform both rotation and scaling as shifts. However, it may cause missing of points when converting images from rectangular coordinates to log-polar coordinates. Hence, interpolation is needed.

By taking care of all three parameters of translation, rotation and scale, input image is transformed [33].

2.3.3 Morphological Pyramid Image Registration (MPIR) algorithm

MPIR algorithm [34] takes low-level features such as edges and corners to define global affine transformation model. MP is able to store multi resolution images and is able to eliminate details and to leave the main features. MPIR uses optimization scheme to minimize the sum of squared errors (SSE) between two images. In each Morphological Pyramid (MP) level, a coarse-to-fine refinement is processed till the convergence criterion is achieved. The SSE is minimized by increasing estimated criterion for each level. Thus, final estimation is achieved through this iterative process.

2.3.4 Classical genetic algorithm

Genetic algorithm (GA) was inspired by Darwin's theory of 'survival of the fitness'. GA is a stochastic process to search the solution space to a specified problem, thus, it is also a standard method to solve the optimized problems. The basic principles of GA were first proposed by Holland in 1975[35]. Medical image registration can be treated as an optimization problem by setting a reference image as a goal to reach or attain.

The optimization process with a genetic algorithm can be viewed as the process flow given in Fig.10.

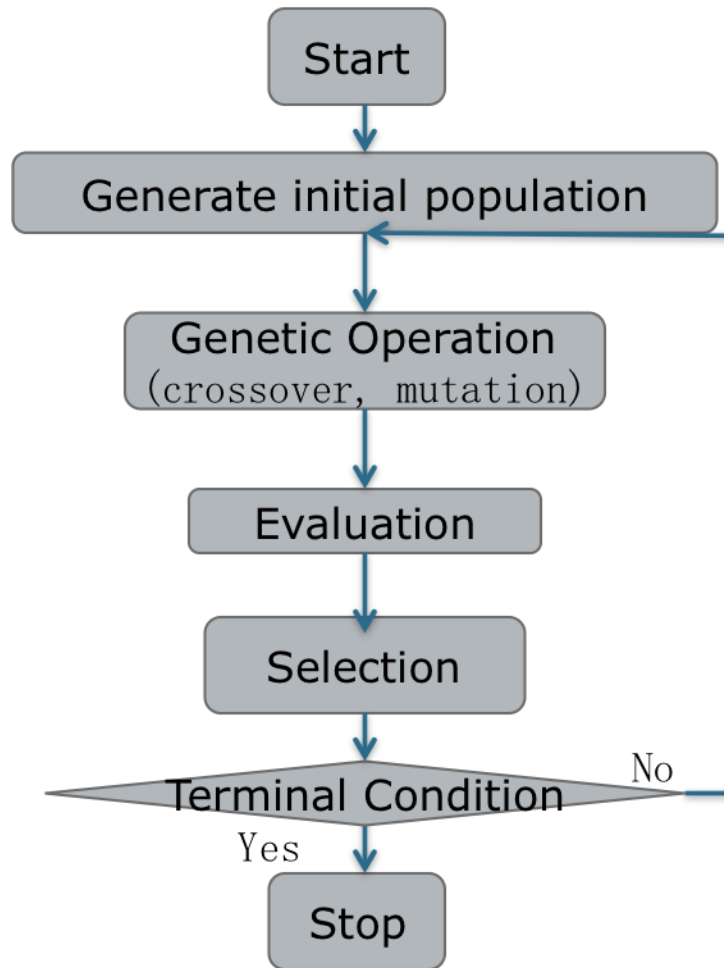


Figure 10: Flow chart of solving problems with Genetic Algorithm.

A sufficiently large population of randomly initialized members is needed so that the solution space is generally covered. A series of processes such as crossover and mutation help to create the next generation. Subsequent generations are created iteratively from previous generations until a stopping criterion is reached. Common terminating criteria [36] are:

1. A solution is found that satisfies the error tolerances.
2. Fixed number of iteration is reached.
3. A highest-ranking solution has plateaued.
4. Manual inspection.

2.3.5 Why GA

There are two requirements for an efficient optimization algorithm: exploration to investigate new search space, and exploitation of existing solutions to generate better solutions. Unfortunately, these two requirements are contradictory. A good research algorithm needs to balance these constraints.

A purely random search is good at exploration but does not address exploitation. Similarly, gradient search techniques focus on exploitation but rarely investigate new solution spaces [37]. According to Holland [28], GA combines both exploration and exploitation well, which makes it an efficient and ubiquitous strategy for optimization problem.

Chapter 3

Genetic Algorithm for image registration

3.1 Genetic Algorithm

Genetic Algorithm (GA) is a search technique that mimics the process of evolution and is widely used in optimization problems. In Genetic Algorithms, a population of initial candidates called parents blends their makeup, i.e. crossover, with the possibility of added mutation to create next generation. Each candidate contains a set of properties called chromosomes. (For this work the chromosomes are the translation and rotation settings of the subject image volume.)

The geometric relationship between two 2-D rigid images can be represented by three parameters, two translational parameters and one rotation parameter. We define a set containing those parameters as a chromosome in this Genetic Algorithm. Each parameter is treated as one gene in chromosome. They are defined as:

	Translation Genes
Dx	Translation of X-axis
Dy	Translation of Y-axis
	Rotation Gene
θ	Rotation about Z-axis

Table 1: Parameters of 2D rigid transformation.

Thus, for 2-D rigid image registration, the transformation matrix can be expressed as:

$$T = Tr \times Rz \quad (12)$$

where,

$$Tr = \begin{matrix} \hat{e} & 1 & 0 & 0 & Dx & \hat{u} \\ \hat{e} & 0 & 1 & 0 & Dy & \hat{u} \\ \hat{e} & 0 & 0 & 1 & 0 & \hat{u} \\ \hat{e} & 0 & 0 & 0 & 1 & \hat{u} \end{matrix} \quad (13)$$

$$Rz = \begin{matrix} \hat{e} & \cos q & \sin q & 0 & 0 & \hat{u} \\ \hat{e} & -\sin q & \cos q & 0 & 0 & \hat{u} \\ \hat{e} & 0 & 0 & 1 & 0 & \hat{u} \\ \hat{e} & 0 & 0 & 0 & 1 & \hat{u} \end{matrix} \quad (14)$$

The Genetic Algorithm approach 1) evaluates and ranks each member of the population retaining only the highest ranked members, 2) an infrequent mutation operator serves the function of expanding the search boundaries randomly, and 3) the crossover takes charge of reproduction by exchanging genes among selected chromosomes.

3.1.1 Selection

Selection is a stage in which parents are ranked within the entire population. According to evolution theory, only those members highly ranked have their genes contribute to the next generation. Generally, the top N highest ranked parents are selected to produce offspring. Selection is processed by the fitness function, which is, in other words, minimum target of the mission. There are different techniques to implement selection in GA such as: tournament selection, steady state selection, ranks selection and so on.

In tournament selection, several tournaments are played among a few individuals. The

individuals are selected randomly. The winner of each tournament will be selected as a parent for making the next generation. Weak individuals have little chance to be selected in large tournament size. This continues until a desired goal reached.

In steady state selection, a few good chromosomes are used for creating new offspring in each iteration. New offspring will take place of the lower ranked chromosomes. The recombined population migrates to the next generation without any more selection.

In rank selection, which is also called elitism, parents are signed as a fitness value via fitness function. Fitness value 1 or as close to 1 as possible will be the general goal for whole evolution process. Whole sets of parents will be ranked according to their fitness values. After ranking, top N ranked objects will be selected as parents.

In this thesis, elitism is selected as the strategy. Potential solutions standing for a measurement of similarity are ranked based on the intensity value of pixels. The formula to evaluate the potential solutions are fitness function that will be discussed in detail later this chapter. In this research, an initial population is set to be 5000 based on randomly normal distribution as:

$$f(x) = \frac{1}{\sigma\sqrt{2\pi}} e^{-\frac{(x-\mu)^2}{2\sigma^2}} \quad (15)$$

where μ is the mean of the distribution and σ is its standard deviation.

This large amount population provides enough search space. Then initial solution are evaluated according to a similar criterion and ranked from high to low related. Then top ranked 200 are selected as parents to generate offspring. This process is iteratively done

till ideal solution is found. In intensity-based registration, potential solution is exactly the transformation model. Thus finding the best solution is in other words finding one transformation matrix by applying which subject image can be aligned to reference image as similar as possible.

3.1.2 Crossover

In this stage, the algorithm allows parallel evolution in the population of N chromosomes. New generations are created as two randomly chosen parents exchanging portion of their chromosome while the exchange point is also selected randomly [43] [38] [39]. Chromosomes past from the last generation are all selected by fitness function, in other word, are all elites. Crossover among such elites can help to generate better chromosomes. Common used crossover strategies are discussed as following:

One-point crossover (Fig. 11a)

In one-point crossover, two mating chromosomes are each cut once at the corresponding point and exchange the sections. [40]

Two-point crossover (Fig. 11b)

In two-point crossover, (or multi-point crossover), chromosomes are regarded as loop. And sections between two cut points are exchanged. According to the researches from DeJong [41], multi-point crossover may reduce the performance of GA.

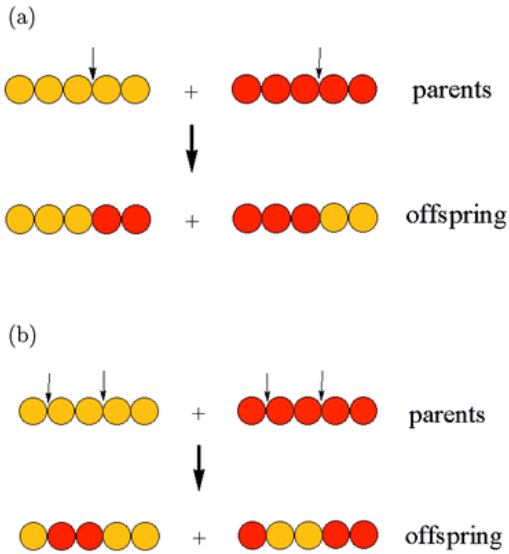


Figure 11: Illustration of one-point (a) and two-points (b) crossover [42].

Uniform crossover

Uniform crossover is significantly different from one-point crossover. It allows exchanges in gene level but not chromosome level. Genes are selected from two parents corresponding to a randomly created crossover mask. Crossover mask is constituted by ‘1’s and ‘0’s, where ‘1’ refers to copying gene from parent 1 and ‘0’ refers to copying gene from parent 2. The process is illustrated as Fig. 12.

Crossover mask	1	0	0	1	0	1	1	1	0
Parent 1	1	0	1	0	0	0	1	1	1
	↓			↓		↓	↓	↓	
Offspring 1	1	1	0	0	0	0	1	1	1
		↑	↑		↑				↑
Parent 2	0	1	0	1	0	1	0	0	1

Figure 12: Uniform crossovers.

In this research, one-point crossover is chosen as the crossover strategy. That means the values of three genes D_x , D_y , q are cut once for each and exchange within each types of gene. For example, $P_1(D_x, D_y, q)$ and $P_2(D_x, D_y, q)$ containing three genes respectively.

Then children are generated from the following formula:

$$C_1 = aP_1 + (1 - a)P_2 \quad (16)$$

$$C_2 = (1 - a)P_1 + aP_2 \quad (17)$$

a is uniformly distributed pseudorandom number changing in different generation between 0 and 1 but is constant within the generation. Again, exchanging of the values is just happen within each types of gene. As mentioned in Chapter 2, Genetic algorithm combines exploration and exploitation very well. It's crossover providing the possibilities to generate better solution. It's mutation help to explore new search space.

3.1.3 Mutation

In Evolution theory, mutation is a change in the DNA sequence. DNA affects how organism behaves, how it looks and its physiology. Thus, a change in DNA may cause changing in all these aspects of the organism. Mutations are essential to evolution since they bring the opportunity of change, independent of the parent DNA. For example, in Fig. 13, new gene is brought into original chromosome, thus coming up with a new chromosome. There are many ways that DNA may be changed. In summary, here are several types of mutation [43,44]:

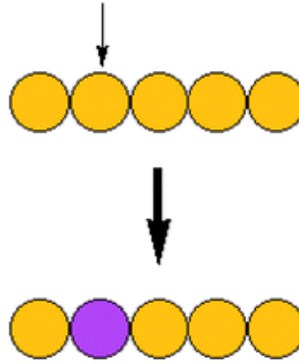


Figure 13: Illustration of mutation [33].

Substitution:

A substitution is an exchange of one codon to another, which may lead to different protein produced. For instance, ‘ABCDEF’ is changed as ‘ABCDFE’ in which letter ‘F’ takes the place of ‘E’.

Insertion:

Insertion means that extra genes are brought to DNA. Such as, ‘ABCDEF’ becomes ‘ABCDEFEE’ in which ‘EE’ is inserted between ‘E’ and ‘F’.

Deletion:

Deletion means that a section or sections of DNA are lost, or in other world, deleted. For example, ‘ABCDEF’ becomes ‘ACEF’ in which ‘B’ and ‘D’ are deleted.

Frameshift:

Since protein-coding DNA is translated three by three, insertions and deletions may cause a shift of codon. In this case, message may mislead. For example, ‘ABC DEF GHI’ may become ‘BCD EFG HI’ since ‘A’ is lost.

Within the physical model there are several reasons for mutations [45,46]. 1) DNA may fail to copy correctly. 2) External influences such as specific chemical or radiation may cause DNA breaks down, in which case, even cell may repairs the DNA, and it cannot do a perfect job to get exactly DNA as before. To simulate this process numerically, several strategies have been proposed.

In numerical GA, mutation has similar meaning as in evolution. Most population-based, reproductive, optimization algorithms face a critical problem called premature convergence problem [47,48,49]. This problem happened when highly suitable parameter existed in current gene pool since early evolution periods. If highly suitable parameter leads to local optima, then new generations be situated will also around the local optima. Crossover can help to generate new chromosomes to avoid premature convergence problem. Mutation is another way to avoid such problems by bringing new gene values to the gene pool. A probability of mutation is introduced in order to give opportunities to generate offspring distant from local optima and potentially higher ranked. Frequently used mutation factors include [50]:

Gaussian

A Gaussian distributed random value is introduced into the chosen gene. The gene need to stay in the upper and lower limits specified by user, or it fails.

Non-Uniform

The frequency of mutation is high at during early generations and decreases in frequency as the generations go by. This mutation operator keeps the population away from local optimal in the early stage. It can only be used for integer and float genes.

Uniform

Similar to Gaussian mutation, a uniform distributed random value takes the place of the chosen gene. It will fail if exceeds viable limits defined by user. Same as Gaussian mutation factor, it can only use for integer and float genes. Same as the previous techniques, it can only be used for integer and float genes.

The mutation rate is not a function of the generations count. In thesis, we used a uniform mutation strategy in which the frequency of mutation is constant in all stages so that can randomly affect any of the genes. Even in late stages, mutation rate do have the possibility to bring better solution. Since all offspring need to be evaluated by fitness function, so there's no need to worry about the possible mislead from mutation in late stages. Reasonable mutation rates are very important since it can help to prevent the population from going completely astray or remaining localized about a few local optima. Mutation rate can be adjusted by the user with realistic default suggestions provided based upon our alignments of rat-brain images but also stay from 0.01% to 0.1%. Too frequent mutation rate will lead Genetic Algorithm to a rough random guess. In this research, mutation rate is set as 0.03%, which means one mutation among 3000 genes. In detail, there are 200 parents in each generation. Each parent contains 3 genes. And

mutation is set to happen each 5 iteration. Hence, every 5 iteration, one of 3000 genes are randomly selected to be placed by a randomly generated value. All random values are based on uniformly distribution.

3.1.4 Fitness function

Fitness function is a criterion quantifying the transformed image match to the reference image. An ideal fitness function can precisely describe the qualification of each candidates fit. Meanwhile, an ideal fitness function should be able to be computed quickly, since to reach the optimization goal numerous generations must evolve. Common used fitness functions for intensity-based image registration are illustrated as following:

Sum of Squares of Differences:

For images A and B (or B') with pixels $M \times N$ and intensity value on each pixel is referred as $A(i, j)$ and $B(i, j)$. B' is the image B after registration.

$$\text{SSD} = \frac{1}{M \times N} \sum_i^M \sum_j^N |A(\mathbf{i}, \mathbf{j}) - B'(\mathbf{i}, \mathbf{j})|^2 \quad \forall \mathbf{i}, \mathbf{j} \in A \cap B' \quad (18)$$

SSD value will be a minimum if two images are exactly aligned and will increase with the misalignment. If small intensity errors between small subject and reference misalignments, SSD is likely to work well. The approach using SSD as the measurement will fail if the intensity data diverges abruptly [51].

Correlation Coefficient

Taking image A as reference image and image B as subject image, B' is the registered image by applying transformation matrix. Intensity value on each pixel is referred as

$A(i, j)$ and $B(i, j)$ (or $B'(i, j)$).

$$\mathbf{CC} = \frac{\sum_{i,j} (A(i,j) - \bar{A})(B'(i,j) - \bar{B}')}{\sqrt{\sum_{i,j} (A(i,j) - \bar{A})^2 \sum_{i,j} (B'(i,j) - \bar{B}')^2}} \quad \forall i \in \mathbf{A} \cap \mathbf{B}' \quad (19)$$

Where \bar{A} and \bar{B}' are the mean values of pixels in image A and transformed image B [52]. It measures the statistical dependence between two images corresponding to intensity values within each pixel. The accuracy of CC as a criterion is validated for rigid body registration for CT, MRI [53]. CC is one when two images are totally same and will decrease when two images are getting less similar.

Ratio Image Uniformity (RIU)

RIU was originally introduced for the registration of serial PET studies. Recently, it was more widely used in MR image registration as well as cross-modality registration between PET and MRI [54] [55] [56] [57]. RIU is calculated over the overlap domain between A and B', where A refers to reference image, B refers to subject image and B' refers to registered subject image.

$$\text{Image ratio } \mathbf{R}(\mathbf{x}) = \frac{\mathbf{A}(\mathbf{x})}{\mathbf{B}(\mathbf{x})} \quad (20)$$

$$\text{Mean value } \bar{\mathbf{R}} = \frac{1}{N} \sum_{\mathbf{x}} \mathbf{R}(\mathbf{x}) \quad (21)$$

$$\text{Standard deviation } \sigma = \sqrt{\frac{1}{N} \sum_{\mathbf{x}} (\mathbf{R}(\mathbf{x}) - \bar{\mathbf{R}})^2} \quad (22)$$

$$\text{Ratio image uniformity } \mathbf{RIU} = \frac{\sqrt{\frac{1}{N} \sum_{\mathbf{x}} (\mathbf{R}(\mathbf{x}) - \bar{\mathbf{R}})^2}}{\bar{\mathbf{R}}} \quad (23)$$

This algorithm iteratively determines the transformation matrix that minimizes the normalized standard deviation.

In this research, correlation coefficient is selected as the fitness function to evaluate the registration result. Thus, the fitness values returned for each potential solution will be expected to be the higher the better.

All in all, checking fitness is a process to select top ranked population among parents and their offspring. Usually the population count remains constant at the original population. The top N ranked parents generate next generation and both sets are ranked together retaining the higher ranked to maintain the original population.

3.2 Implementation

3.2.1 Data Sets

The images are represented digitally as sets of cubic matrix of numbers representing the intensity value in each place. The data we are working on in this research are MRI (Fig. 14) and fMRI (Fig. 15) volumes of rat head. Dimension of data sets will be listed out in Chapter 5. The algorithms are able to select slice and number of time step so that user can pick up two images looks most similar.



Figure 14: One slice of MRI volumes of rat brain, at a size of 256x256.

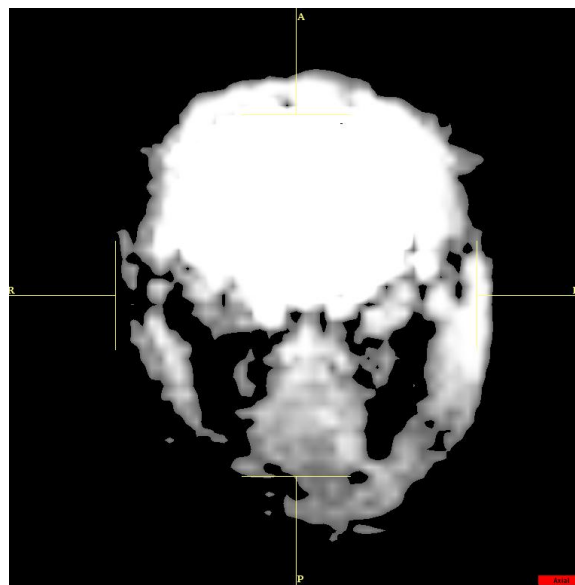


Figure 15: One slice of fMRI volumes in a specified time step, at a size of 64x64.

3.2.2 Preprocessing

According to our test results of rat brain image registration, the GA algorithm can achieve quality alignments based on original images. However, cropped images can help GA reach alignment in shorter times eliminating unnecessary regions and reduction of

calculations. For brain images, the real interest region is the brain tissue area not the skull. For example, the region within the red circle will be the region of interest (as Fig. 16), while the outside region will be unconsidered area.

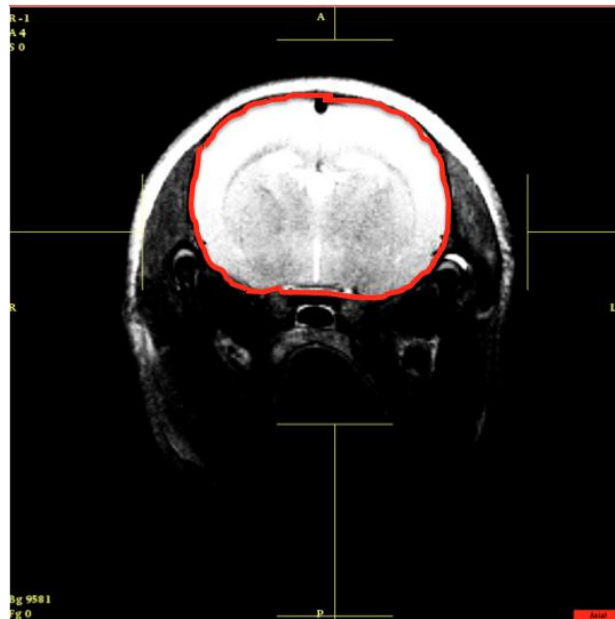


Figure 16: Region of interested marked within red circle.

Calculation on original images will take the unconsidered area into account. Those unnecessary areas can mislead the similarity which in other word may accidently have high similarity but actually not looks similar at all. Therefore, before start the GA registration, we allow user pick out the region of interest from both reference and subject image into two same-sizes smaller square. As long as the procedure of crop has done, GA registration will take the generated matrix containing intensity value of each pixel into account.

3.2.3 GA registration

To start a GA registration, the user needs to define the initial population count. Each generation will maintain the same number of population (For example, N). For 2D rigid registration, there are chromosomes each containing three genes among each population constructing transformation matrix. In crossover step, from first ranked chromosome, another chromosome was randomly selected to make one-point exchange in sequence. Each two chromosomes make two new chromosomes. Thus, after crossover, we will have $2N$ chromosomes in total. A common problem with many genetic algorithms is cloning. This work avoided the situation by using the ‘unique’ function within MATLAB. Parents with the same chromosome are reduced to one. With only unique candidates the population is ranked according to fitness function, and top N candidates are selected as parents for crossover to create the next generation. Between crossover and fitness selection, there is always a probability of mutation. Normally, mutation rate will be no larger than $1/1000$. However, according to my research, mutation rate can be much more frequent in order to mitigate local optima isolations.

3.3 Sample results

In order to evaluate the performance of GA registration and to make image registration easier to operate, a user-interface (UI) (will be introduced in Chapter 4) was designed for the registration. Several functions are placed on this UI to enhance the GA performance, such as: buttons for cropping; running and stopping, editable text for user-defined information, dynamic plots and so on. Besides the necessary preprocessing functions (will be discussed in Chapter 4), this package parses all the parameters to the GA routine

discussed previously. As a sample presenting how the addressed GA preformed, we did 2D rigid registration on two MR images of rat brain in the size of $256 \times 256 \times 18 \times 1$.

Image information is shown as following:

	Slice number	Time step
Reference image-WKY1	6	1
Subject image-WKY2	6	1

Table 2: Image information in sample test.

Fig. 17 shows the overlap view of reference image (bottom) and subject image (top) before (a) and after (b) GA registration. From the zoom-in view of both overlaid images, we can see a better alignment after registration.

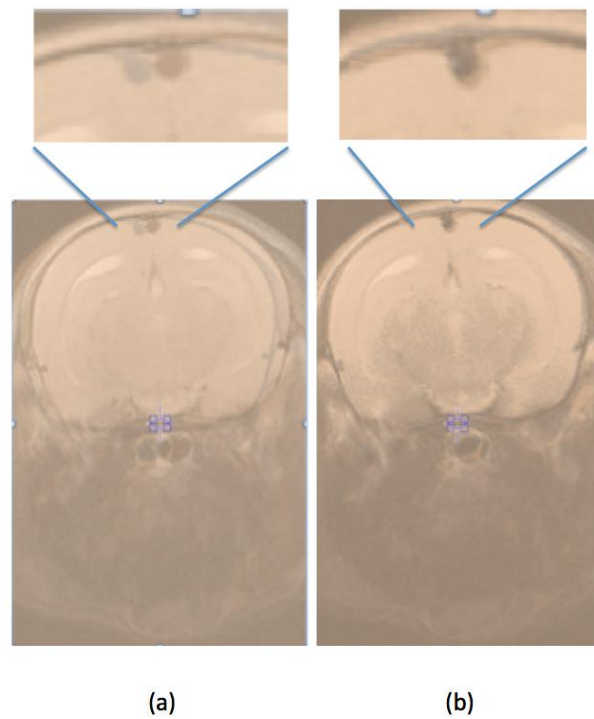


Figure 17: View of images before (a) and after (b) registration.

After about 3 minutes, the correlation fitness function approached to 0.83 with a 1.0 being an identical match. Compared to the gold standard alignment strategy (manual alignment) the GA accuracy reached 96.5%, where accuracy is defined as:

$$\mathbf{Accuracy} = \frac{\mathbf{Correlation\ between\ GA\ registrated\ images}}{\mathbf{Correlation\ between\ manually\ registrated\ iamges}} \quad (24)$$

Accuracy describes the performances of GA by comparing with manually registration since manually registration plays a critical role in image registration and is reliable in most cases. Thus, a comparative correlation of GA performance is also reliable and can meet the requirement of further analysis.

During the interactive iteration process, axes located on the right panel of UI will display in real time the changing correlation fit and its history. According to such real time display, user may choose to override the process and stop it. Or, program will stop when any one of evaluation criteria (introduced in Chapter 2) is reached.

Another sample test was done between ratbrain01 as reference image and ratbrain03 as subject image.

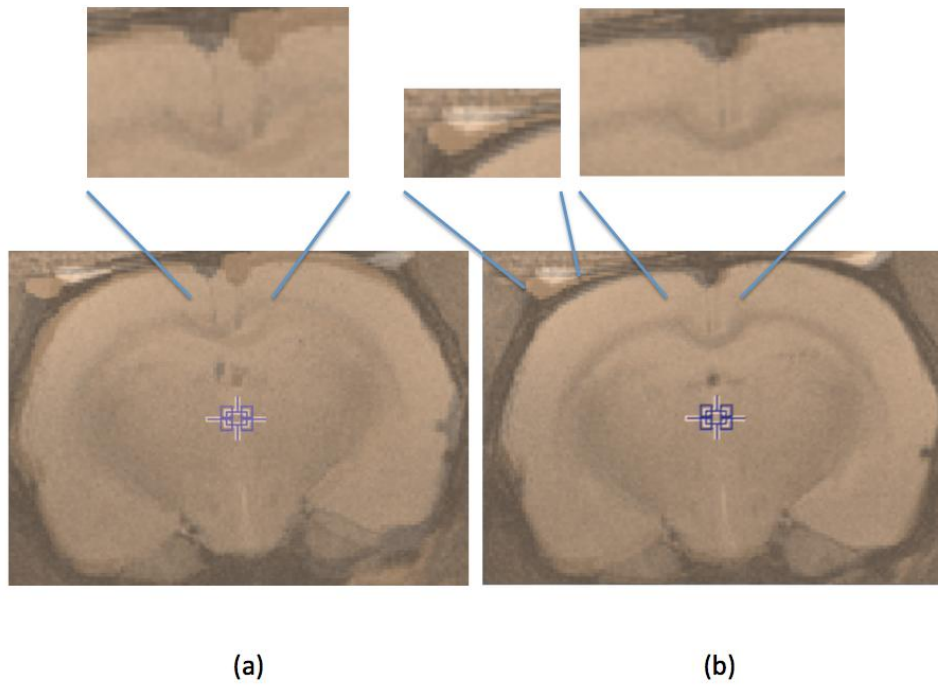


Figure 18: View of comparison between before (a) and after (b) registration.

From Fig. 18, we can tell the region of interest, which is the brain tissue, is aligned well. In Fig. 18 (b), we can still notice the small piece of white region (zoomed in on top middle) in upper left corner from subject images is still not aligned with same region from reference image. However, this small region is not our RIO. More detailed comparison in accuracy between GA and manual operation is provided in Chapter 5.

Chapter 4

MATLAB GUI

4.1 Why GUI

Though command line is frequently used and is able to do image alignment, a Graphical User Interface (GUI), or UI, is a great tool for image registration. New users can pick up the interface much easier than command line use since it's more clear and visualized. Though command line can perform more various operations, for image registration using genetic algorithm, a well-designed GUI can meet all the user needs. Typically, a GUI contains one or more controls by components that enable the user to perform interactive operations such as mouse click and keyboard typing. As a result of setting up controls with Layout Editor, GUIDE automatically generates a template controlling the behaviors and functionality of the elements of GUI. The structure of application is generated as an m-file. Properties and behaviors of all components such as toolbars, menus, sliders and other controls were defined and called via callback functions that can be programmed within MATLAB. The callback function is triggered by particular user action such as pressing a button, mouse click, selecting an item, moving a slider bar, and so on.

4.2 Screen Sketches

According to the controls demanded for GA registration as previously discussed, a user friendly interface with three panels controlling registration type (upper left panel), inputs (lower left panel) and outputs (right panel) was designed as Fig. 19.

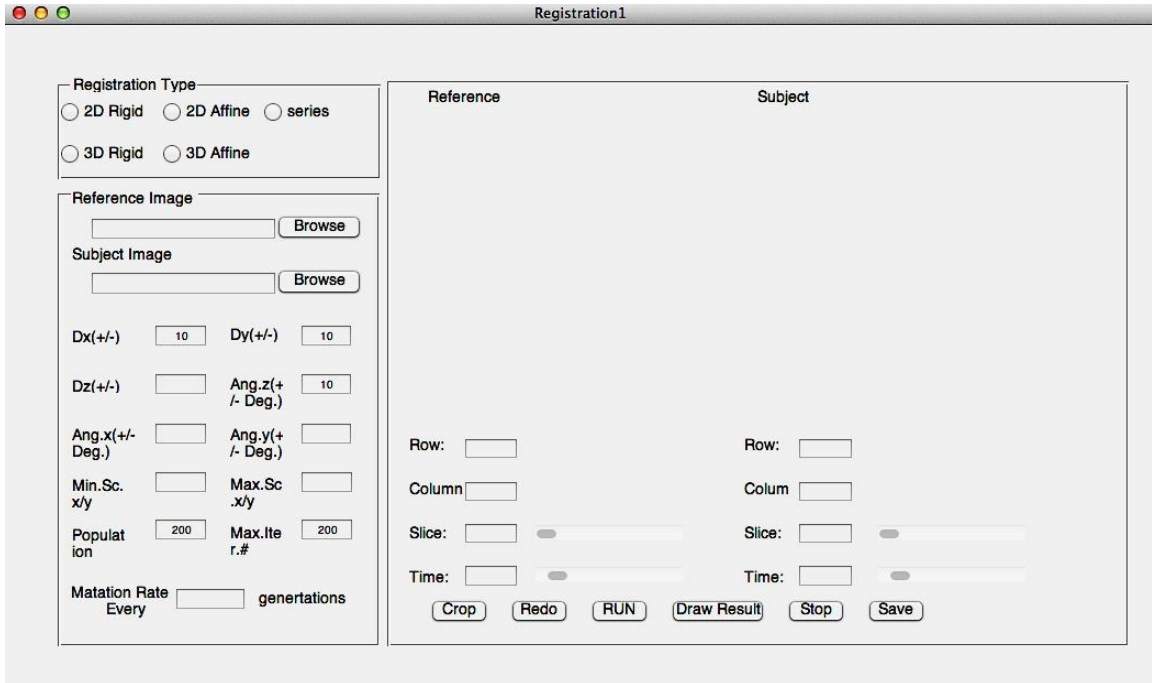


Figure 19: User interface for 2D rigid registration with genetic algorithm.

A flowchart showing procedures are displayed as Fig. 20.

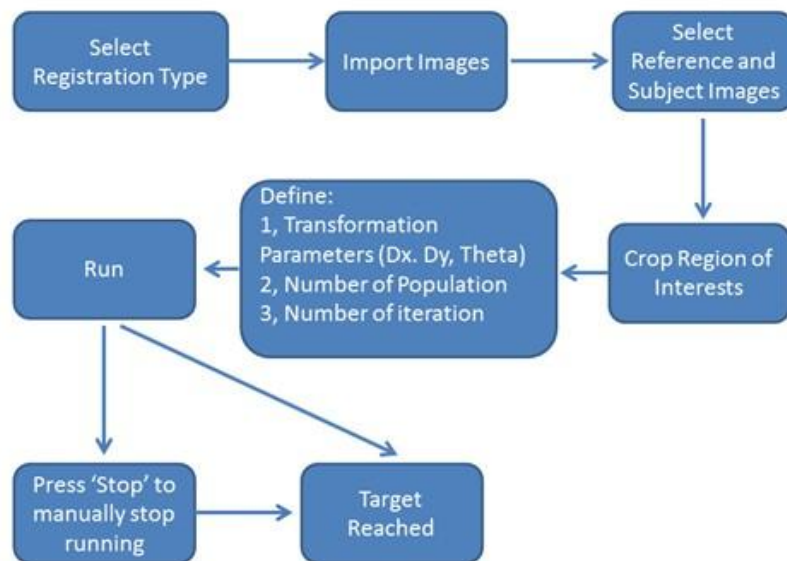


Figure 20: Operation direction.

Each step is introduced as follows:

Select registration type

Though only 2D rigid registration is implemented in this research, to make this GUI a start for well-developed image registration tool, other options for further work are also built. In lower left frame, selectable texts will be visible or invisible depending on which registration type is chosen and whether or not the function has been incorporated. Again for this work, the 2D rigid registration was designed, built and tested. Thus, registration type needs to be selected as first step (Fig. 21).

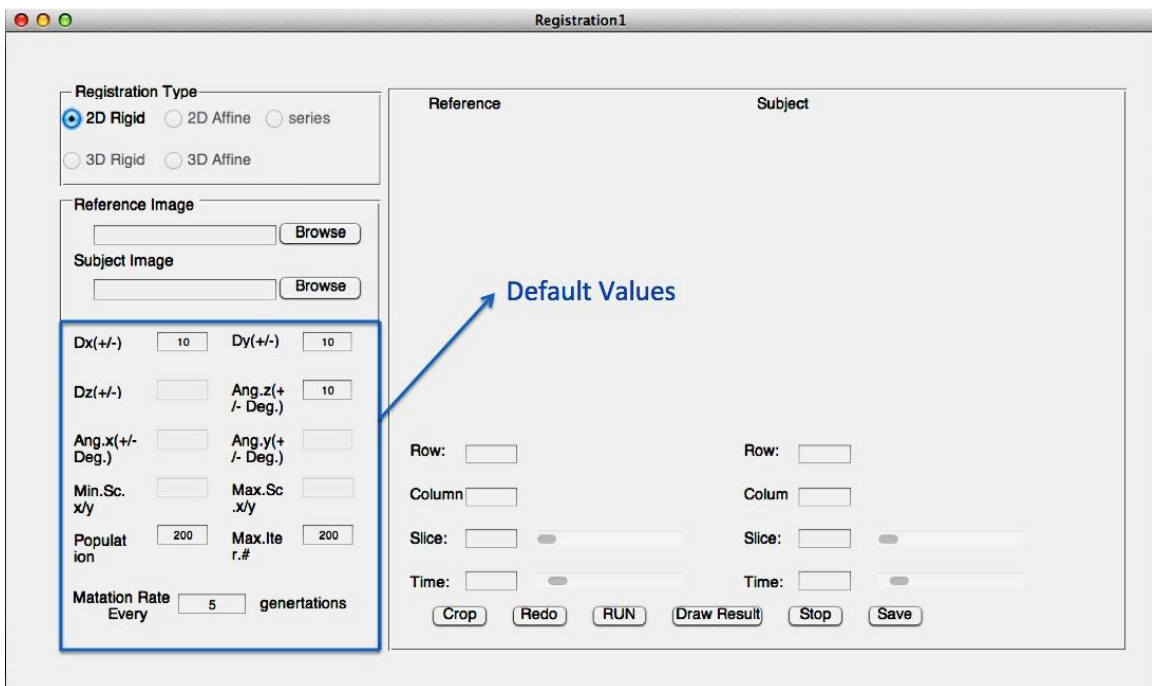


Figure 21: Selecting registration type.

On the left bottom corner, there are all kinds of editable text that are necessary for image registration operation, such as translation and rotation parameters, populations, maximum number of iteration, and mutation rate. If the parameters are not changed by the user, GA will use default values: in-plane translation Dx and Dy are set within $\pm 10\%$ of lineal

span; in-plane rotation angle is set within +/-10 degrees. The unit for axial window is set to be pixel. A pixel is a physical location or the smallest element in raster image. The address of pixel corresponds to its physical coordinates and the value on each pixel corresponds to its intensity. In this GUI, the size of axial window is set to be 256 × 256 pixels, in which case, user can define transformation according to the visual comparison between two cropped images by imaging rows and columns are both divided into 256 cells.

As mentioned in Chapter 3, mutation rate is set to be 0.03% in this research. Thus, mutation happened every 5 generation. Even though, mutation can help to explore more search space, high frequent mutation will turn Genetic Algorithm to be a rough random guess.

The population here is set to be 200 as default and is different from the initial population that is 5000 as mentioned in Chapter 3. The ‘population’ here means the constant number of population in every generation.

Maximum number of iteration is default to be 200 since in the experiments, genetic algorithm usually converging before 200th iteration.

Browse input images

To import reference and subject images, user could click ‘Browse’ in lower-left frame as shown in Fig. 18. Current program has a limitation that file-type need to be ‘.spr’ or ‘.sdt’. Images will be displayed in the right panel, respectively. Meanwhile, the dimension information about number of rows, columns, slices, time steps are shown in edit box separately.

Slide sliders to view slices

Two sets of slider bars are built in this GUI taking responsible for switching the slices allows user to view tomographic slices interactively and to ensure proper orientations (Fig. 22). For anatomy images, there is only one time step. However, for functional images there are generally numerous time steps. (Functional imaging is the time history of the volume being recorded.) Thus, depending on different situation, it's necessary to adjust slice and/or time.



Figure 22: Switching slices by using slider bars.

Crop region of interests

‘Crop’ and ‘Undo’ button allow user to crop out the region of interest. By clicking ‘Crop’, there is a small cross appearing in the middle of reference image (as shown in Fig. 23). Stretch and adjust the cross till the rectangle surrounds the region of interest and then double click. Then, there is a pop-up message informing user to define the left upper corner of subject image in order to crop it with the same size as reference image.

Meanwhile, GUI provides horizontal and vertical line as reference to assist user decide the upper left corner. If the cropped subject image shows to be unsatisfactory. The ‘Undo’ button allows user go back to crop stage and redo crop all over again.

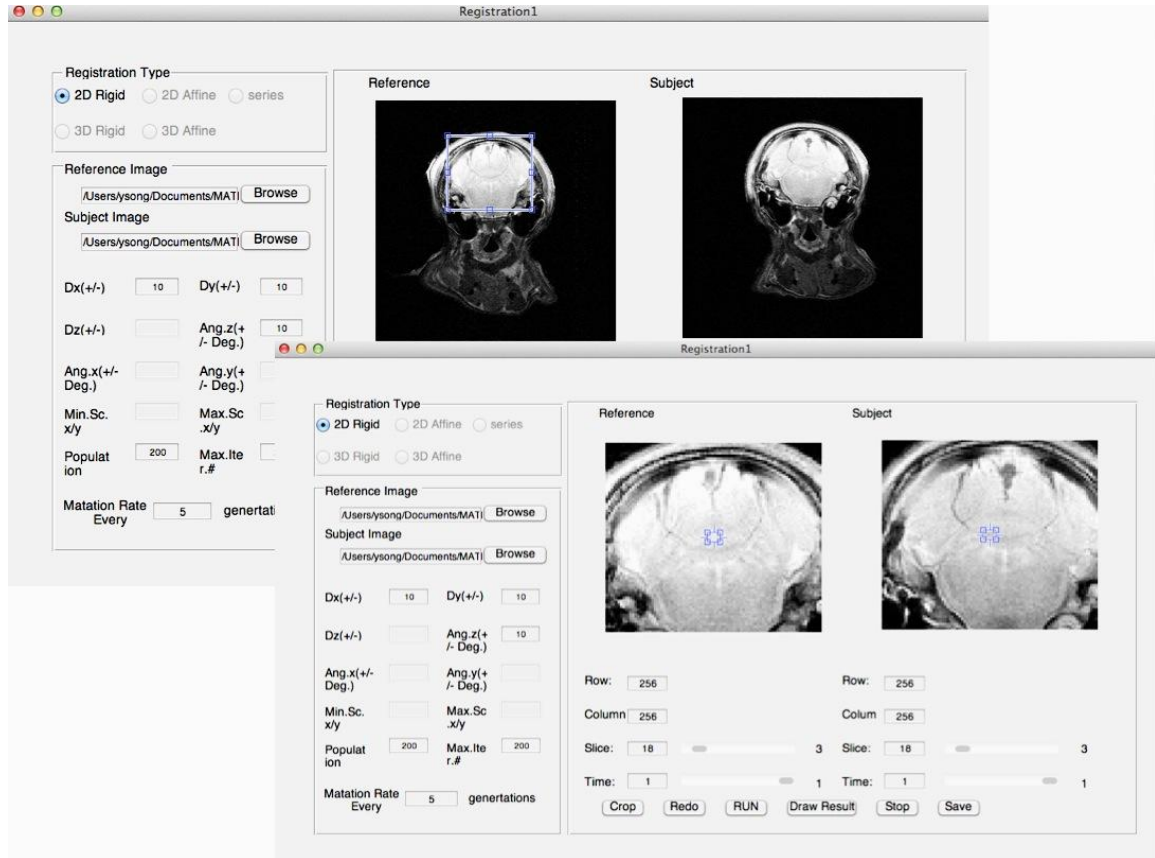


Figure 23: Cropping reference and subject images.

Start to register

As the last step, before starting the registration, user needs to define the population count and maximum iteration number. The population count remains constant in each generation and maximum number of iterations determines the maximum number of generations created. After completing these steps, we are ready to do the registration. As shown in Fig. 24, by hitting ‘Run’, calculation starts. At the same time, highest

correlation in each generation and the growth rate of correlation will be displayed on the right-hand-side display window (marked as blue rectangular).

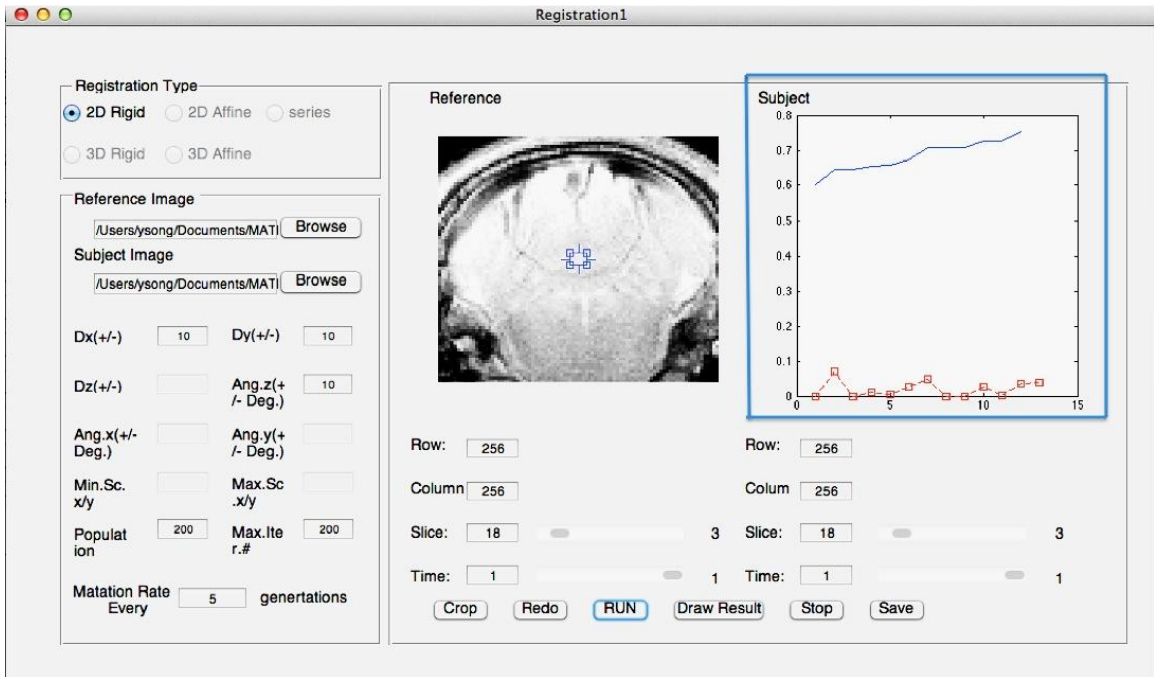


Figure 24: Display of correlation and growth rate of the changing of correlation between reference and subject images.

Convergence evolution and stop

The iteration process can be stopped by either manual intervention, exceeding the maximum specified iterations or automatically based on a convergence criterion. In this program, an automatic convergence criterion was set to be the maximum range of correlation values over a span of 10 generation to be less than a specified tolerance. This convergence check is set to start at $\frac{1}{4}$ of the maximum iteration. Additionally, if the correlation exceeds 95%, the program will also stop since a 95% correlation value will satisfy all alignment requirements. Thus, once this goal is reached, there's no need to continue the approaching process.

Once the iteration process terminates, hit 'Draw result' button and the registered image will be displayed in right-hand-side window so that user can visually check the alignment. Transformation matrix, registered images and crop information are outputted as ASCII text file to the same folder. This program can be run repeatedly by executing a MATLAB script so that all subjects within a folder undergo the alignment process.

Chapter 5

Results

In previous chapters, we described the background, theory and implementation of an alignment strategy using a genetic optimization algorithm for 2D rigid body registration. In this chapter, registration results based on this system are presented. The quality of GA registration is presented by compared to manual operation based on MIVA (Medical Image Visualization and Analysis) [58]. This algorithm using the interactive MATLAB GUI does not require much user intervention and expedites the alignment process for which many technicians are ill-trained to perform effectively. Additionally, it takes less time to run the GA than manual operation. The ability to align in batch mode allows the scientist/technician to perform other research tasks.

5.1 Summary of terms

GA- 2D rigid body genetic algorithm with 3 chromosomes (dx, dy, and rotation angle)

GS – gold standard, performed by skilled user with software MIVA

Accuracy - the quality of GA registration results compared to result from GS

WKY1, 2, 3 anatomy images of rat brain subjects 1, 2, and 3 obtained from University of Massachusetts Medical School's Center for Comparative NeuroImaging, (CCNI).

RatBrainVol01, 02, 03... - anatomy images of rat brain subjects 01, 02, 03... Also obtained from CCNI.

5.2 Data sets

Source image information is listed in Table 3 and Table 4. In this research, different kinds of alignments were performed including inter-subjects, intra-subjects, functional and anatomical volumes, which are all in the axial orientation with int16 data type, and little endian.

Image	Dimension (row, column, slice, time)	FOV(mm) (row, column, slice, time)
WKY1	$256 \times 256 \times 18 \times 1$	$32 \times 32 \times 18 \times 1$
WKY2	$256 \times 256 \times 18 \times 1$	$32 \times 32 \times 18 \times 1$
WKY3	$256 \times 256 \times 18 \times 1$	$32 \times 32 \times 18 \times 1$
ratBrainVol01	$256 \times 256 \times 12 \times 1$	$30 \times 30 \times 14.4 \times 1$
ratBrainVol02	$256 \times 256 \times 12 \times 1$	$30 \times 30 \times 14.4 \times 1$
ratBrainVol03	$256 \times 256 \times 12 \times 1$	$30 \times 30 \times 14.4 \times 1$
ratBrainVol04	$256 \times 256 \times 12 \times 1$	$30 \times 30 \times 14.4 \times 1$
ratBrainVol05	$256 \times 256 \times 12 \times 1$	$30 \times 30 \times 14.4 \times 1$
ratBrainVol06	$256 \times 256 \times 12 \times 1$	$30 \times 30 \times 14.4 \times 1$
ratBrainVol07	$256 \times 256 \times 12 \times 1$	$30 \times 30 \times 14.4 \times 1$
ratBrainVol08	$256 \times 256 \times 12 \times 1$	$30 \times 30 \times 14.4 \times 1$
ratBrainVol09	$256 \times 256 \times 12 \times 1$	$30 \times 30 \times 14.4 \times 1$
ratBrainVol10	$256 \times 256 \times 12 \times 1$	$30 \times 30 \times 14.4 \times 1$
ratBrainVol11	$256 \times 256 \times 12 \times 1$	$30 \times 30 \times 14.4 \times 1$
ratBrainVol12	$256 \times 256 \times 12 \times 1$	$30 \times 30 \times 14.4 \times 1$
ratBrainVol13	$256 \times 256 \times 12 \times 1$	$30 \times 30 \times 14.4 \times 1$

Table 3: Source anatomical images.

Functional Image	Dimension (row, column, slice, time)	FOV(mm) (row, column, slice, time)
WKY1	$64 \times 64 \times 18 \times 200$	$32 \times 32 \times 18 \times 200$
WKY2	$64 \times 64 \times 18 \times 200$	$32 \times 32 \times 18 \times 200$
WKY3	$64 \times 64 \times 18 \times 200$	$32 \times 32 \times 18 \times 200$

Table 4: Source functional images.

5.3 Application for functional image registration

In the cases of brain tumor treatment, resection, radiation therapy, patients need to be imaged repeatedly in order to track the therapeutic (or not) treatment progress. The application of registration in these longitudinal studies is necessary to evaluate the structural and functional changes that may occur. By comparing these registered images, lesion growth, tumor removal, or successful treatment can be quantified. These situations are generally regarded as intra-registrations. In traditional manual registration, when a registration within fMRI images is needed, the user usually conducts the registration on anatomy images (higher resolution), since the anatomical images and functional images are taken during the same imaging session. But when lacking of synchronous anatomical images, functional images are rarely aligned successfully given the low quality of images are too blurry. However, functional images registration requires high accuracy since a single pixel error can be marked as a change of disease or treatment. In this case, computer based analysis and registration has the advantage over visualization registration since that whole process is based on intensity values. Results of comparison among functional images through time are shown in Table 5. Note, an accuracy exceeding 100%

indicates that the quantitative alignment using the GA system was more accurate than that obtained by a skilled anatomist using manual alignment techniques.

$$Accuracy = \frac{Correlation\ from\ GA}{Correlation\ from\ GS}$$

Subjects	Time(minutes)		Accuracy
	Manual	GA	
WKY1(RS1)-WKY2(RS1)	5	0.321	102.45%
WKY1(RS1)-WKY3(RS1)	4	0.337	100.5%
WKY2(RS1)-WKY3(RS1)	4	0.327	104.39%
WKY1(RS1)-WKY1(RS2)	5	0.33	103.1%
WKY2(RS1)-WKY2(RS3)	4	0.34	92.1%

Table 5: registration results of functional images.

5.4 Application for anatomical image registration

The purpose of anatomical images registration is to reduce the anatomical differences between images scanned from different subjects. Except for providing a transformation map for functional images, another important application of inter-subject registration is ‘image understanding’. In image understanding, subjects are registered to a template or atlas so that the higher order information of subjects such as structural boundaries, location of anatomical landmarks can be obtained by compared to the template. In our test, WKY1 is chosen to be the template that WKY2 and WKY3 are registered to, and ratBrain01 is chosen to be the template that rest rat brain images are registered to. Taking

WKY sets as example, each subject has a transformation matrix that aligns the volume to that of WKY1. Then WKY1 is aligned to an atlas and using the two alignment matrices, each of the other subjects gets aligned to the atlas.

Subjects	Time(minutes)		Accuracy
	Manual	GA	
WKY1-WKY2	15	2.77	96.5%
WKY1-WKY3	12	2.58	98.47%
WKY2-WKY3	15	3.15	93%
ratBrainVol01-ratBrainVol02	12	2.74	101%
ratBrainVol01-ratBrainVol03	10	2.94	99.2%
ratBrainVol01-ratBrainVol04	9	1.5	91.6%
ratBrainVol01-ratBrainVol05	7	2.69	100%
ratBrainVol01-ratBrainVol06	10	4.37	94.02%
ratBrainVol01-ratBrainVol07	8	2.57	91.6%
ratBrainVol01-ratBrainVol08	9	3.94	100.9%
ratBrainVol01-ratBrainVol09	9	3.4	101.4%
ratBrainVol01-ratBrainVol10	8	2.1	99.2%
ratBrainVol01-ratBrainVol11	8	1.68	99.6%
ratBrainVol01-ratBrainVol12	7	3.88	108.9%
ratBrainVol01-ratBrainVol13	9	2.63	100.23%
ratBrainVol01-ratBrainVol14	9	2.46	99.9%
ratBrainVol01-ratBrainVol15	6	4.27	100%
ratBrainVol01-ratBrainVol16	7	2.76	108.56%

Table 6: registration results of anatomical images.

The time cost of GA varies since it is related to the similarity between the reference and subject images after cropped. The more similar, the shorter time GA needed to converge. Thus, GA does ask for a well performed preprocess. As we discussed in Chapter 4 that, when cropping, GUI provides lines of reference and undo function, which can efficiently improve the preprocessing performance.

If take a look at the results in Table 6, we can find significant time savings and in some cases, the GA provided more accurate results compared to manual operations.

5.5 Failures

Some subject alignments using the GA were not successful. Those failures were caused by a variety of reasons such as low quality of image (one example is shown as Fig. 25) or distinct differences between reference and subject images (such as images shown in Fig. 26)

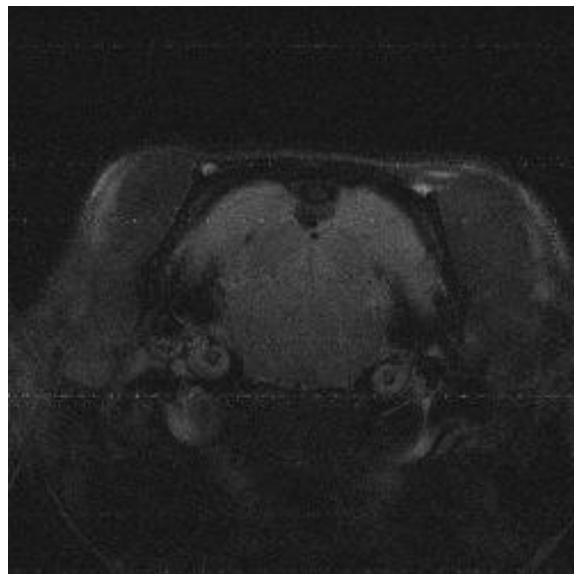


Figure 25: an example of low quality images.

Noise in figure 22 may cause error when calculating the correlation coefficient. Furthermore, this error may mislead the fitness function to keep the low quality alignment while abandon the actual high quality chromosomes.

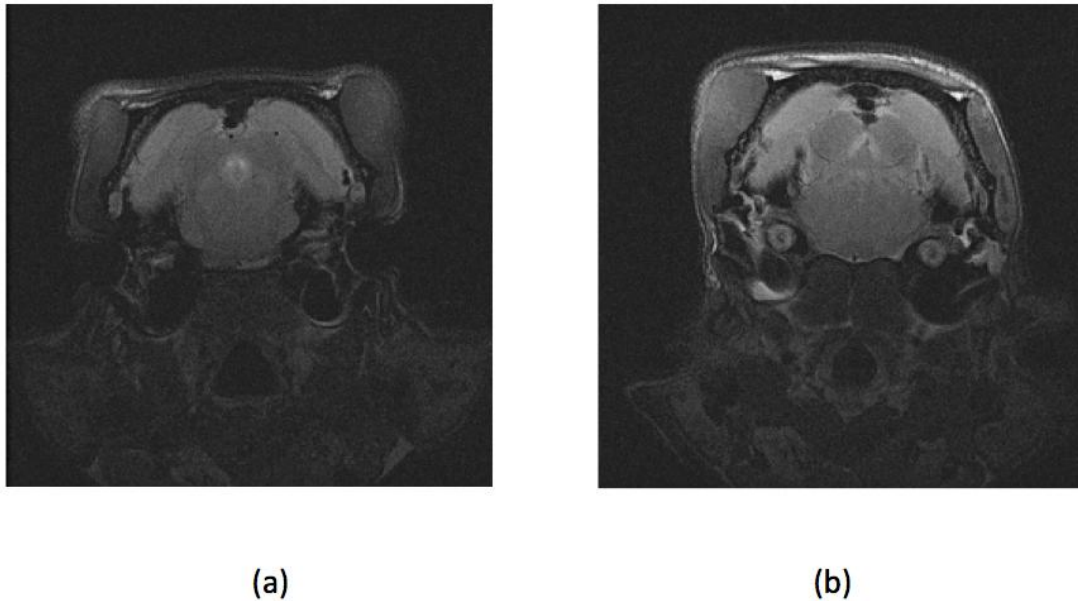


Figure 26: example of two images having distinct different. (a) ratBrainVol01 and (b) ratBrainVol16.

In Fig. 23, we can see image (a) and image (b) have big differences in their shape. The initial correlation coefficient is 0.4613, which indicates that they are very low related. Thus, even after GA registration, correlation coefficient is still lower than 0.6. In such cases, alternate registration strategies may be needed or the image volume collected might be discarded as unacceptable. The GA alignment strategy developed for this work centered on the alignment of rat-brain volumes. The overall consistency of these subjects was incredibly high compared to the differences recorded in human brain image volumes, for example. Consequently, the 2D rigid body alignment strategy applied to the entire volume streamlines the user tasks and provides an effective alignment methodology.

Chapter 6

Conclusions

This thesis developed an automatic image registration tool by using a genetic algorithm optimization strategy housed within an interactive MATLAB GUI interface. Volumes of MRI data collected from UMASS CCNI were used to performance and evaluate the registration system. Compared to traditional manual registration, this automatic image registration system was shown to yield excellent accuracy and reduce the user time efforts significantly.

In this thesis, the method of registration is based on intensity value differences of the entire image or sub-area, compared to fiducial registration strategies. This GA alignment was most effective in functional MRI registrations that lack fiducial details and foil many technicians performing manual alignments.

Genetic algorithm was selected as the optimization strategy:

1. Each generation was generated by crossover pairings of highly ranked parents facilitating good genes to be passed with the hope of better genes resulting through mating.
2. The mutation factor helps to avoid local optima and helps approach an alignment faster.
3. Minimizes the required user preprocessing.

However, certain preprocessing such as crop may enhance the performance of GA. Considering the demands of a better performance GA, we developed a GUI which can

help to accomplish pre-processing, processing, and post-processing of 2D rigid image registration.

In the test result, we can state that the GA alignment provided a highly accurate result compared to manual registration with reduced time costs.

References

- [1] M. P. Wachowiak, R. Smolikova, Y. F. Zheng, J. M. Zurada, and A. S. Elmaghraby. (2004) An approach to multimodal biomedical image registration utilizing particle swarm optimization, *IEEE Trans. Evol. Comput.*, vol. 8, 289–301.
- [2] Antoine Rosset, L. S. (2004). An Open-Source Software for Navigating in Multidimensional DICOM Images. *Journal of Digital Imaging*.
- [3] Basant K Puri, Sam B Hutton, Nadeem Saeed, Angela Oatridge, et al. (2001). A serial longitudinal quantitative MRI study of cerebral changes in first-episode schizophrenia using image segmentation and subvoxel registration, *Psychiatry Research: Neuroimaging*, Volume 106, Issue 2, 141-150.
- [4] L. J., Wang, F., Chen, L. M., Li, R., Advison, M. J., et al. (2011). Automated longitudinal registration of high resolution structural MRI brain sub-volumes in non-human primates. *Journal of Neuroscience Methods*, 99.
- [5] Woods, R. P., Grafton, S. T., Watson, J. D., Sicotte, N. L., et al. (1998). Automated Image Registration: II. Intersubject Validation of Linear and Nonlinear Models. *Journal of Computer Assisted Tomography*, 153-165.
- [6] Ardekani, Bakak A., Alvin H. Bachman, Stephen c. Strother, Yasuhisa Fujibayashi, and Yoshiharu Yonekura. (2004) Impact of inter-subject image registration on group analysis of fMRI data. *International Congress Series*. 49-59.
- [7] Henn, Stefan, Lars Homke, and Kristian Witsch. (2004). Lesion preserving image registration with applications to human brains. *Mathematisches Institute, University of Dusseldorf, Germany, Computer Science Volume 3175*, 496-503.
- [8] Brett, Matthew, Alexander P. Leff, Chris Rorden, and John Ashburner. (2010). Spatial normalization of brain images with focal lesions using cost function masking. *NeuroImage* 14, 486-500.
- [9] Smith, Stephen M., Mark W. Woolrich Mark Jenkinson, and Christian F. Beckmann et al. (2004) Advances in functional and structural MR image analysis and implementation as FSL." *NeuroImage*, 208-219.
- [10] Source: <http://www.rad.upenn.edu/sbia/software/dramms/tutorials/BrainWithLesion.html>
- [11] Raj Acharya, Richard Wasserman, Jeffrey Stevens, and Carlos Hinojosa. (1995). *Biomedical Imaging Modalities: A Tutorial*. *Computerized Medical Imaging and Graphics*, 3-25.
- [12] Hiriyannaiah, H. P. (1997). *X-ray Computed Tomography for Medical Imaging*. *IEEE Signal Processing Magazine*, 42-59.
- [13] Source: <http://www.fda.gov/radiation-emittingproducts/radiationemittingproductsandprocedures/medicalimaging/medicalx-rays/ucm115318.htm>
- [14] Source: <http://www.upmc.com/services/imaging/services/women/services/ultrasound/pages/obgyn-ultrasound.aspx>
- [15] Source: <http://www.osti.gov/accomplishments/pet.html>

-
- [16] Wikipedia. (n.d.). Retrieved Aug. 2013, from http://en.wikipedia.org/wiki/Magnetic_resonance_imaging
- [17] Scholarpedia. (n.d.). Retrieved Oct. 1st, 2013, from http://www.scholarpedia.org/article/Functional_magnetic_resonance_imaging
- [18] Source: <http://cognitiveconsonance.wordpress.com/2013/05/14/neuroimaging-part-2-the-bold-fmri/>
- [19] Daniel N. Rockmore and Dennis M. Healy, Jr., ed. (2002). Modern Signal Processing. Cambridge: Cambridge University Press, Vol. 46,161-184.
- [20] Source: <http://www.imt.uni-luebeck.de/?id=92>
- [21] Anand Rangarajan, Haili Chui, James S. Duncan. (1999) Rigid point feature registration using mutual information, Medical Image Analysis, Volume 3, Issue 4 , 425-440
- [22] C. Studholme, D.L.G. Hill, D.J. Hawkes. (1996). Automated 3-D registration of MR and CT images of the head, Medical Image Analysis, Volume 1, Issue 2, 163-175
- [23] David C. Van Essen.(2004). Surface-based approaches to spatial localization and registration in primate cerebral cortex, NeuroImage, Volume 23, 97-107
- [24] Kostelec, Peter J., and Senthil Periaswamy. (2003) Image Registration for MRI. ,MSRI Publications, 161-184.
- [25] Fitzpatrick, J. Michael, and Milan Sonka,(2000). Handbook of Medical Imaging, Volume 2. Medical Image Processing and Analysis.
- [26] B.S.Reddy and B.N.Chatterji, (1996). An FFT-based technique for translation, rotation and scale invariant image registration, IEEE Transactions on Image Processing, 1266 – 1271
- [27] Ch. Venkateswara Rao, K. M. M. Rao, A. S. Manjunath, and R. V. N. Srinivas. (2004), Optimization of automatic image registration algorithms and characterization, Proceedings of the ISPRS Congress, 698–702
- [28] Leila M.Fonesca and Max H.M.Costa, (1997). Automatic Registration of Satellite Images ,Proceedings on IEEE transaction of computer society, 219-226.
- [29] Sharman, R., Tyler, J. M., & Pianykh, O. S. (2000). A fast and accurate method to register medical images using Wavelet Modulus Maxima. Pattern Recognition Letters, 21 (6-7), 447-462.
- [30] Source: <http://www.robots.ox.ac.uk/~jmb/lectures/TransformLectures.pdf>
- [31] De Castro E, and Morandi C, (1987). Registration of translated and rotated images using finite Fourier Transforms, IEEE Trans. PAMI-9, 5, 700-703.
- [32] Chatterji, B. S. (1996). An FFT-Based Technique for Translation,. IEEE Transactions On Image Processing, 1266-1271.
- [33] A. Averbuch and Y. Keller, (2002). FFT based image registration, Proc. IEEE ICASSP 2002.
- [34] Zhongxiu Hu and Scott T.Acton, (2000). Morphological Pyramid Image Registration” 4th IEEE south west symposium 2000. 227.
- [35] J.H. Holland. (1997). Adaptation in Natural and Artificial Systems. MIT Press.
- [36] Ingole, V. T., C.N. Deshmukh, Anjali Joshi, and Deepak Shete. (2009). Medical image registration using genetic algorithm. Emerging Trends in Engineering and Technology (ICETET). 63-66.

-
- [37] Beasley, D., D.R. Bull, and R.R. Martin. (1993). An Overview of Genetic Algorithms: Part I, Fundamentals, *University Computing* 15, 58–69.
- [38] J.-J. Jacq and C. Roux, (1995), Registration of 3-D images by genetic optimization, *Patt. Recognit, Lett.*, vol. 16, no. 8, 823-841
- [39] D. E. Goldberg, (1989). *Genetic Algorithms in Search, Optimization, and Machine Learning*: Addison-Wesley
- [40] Srinivas, M., Patnaik, L.M. (1994). Genetic Algorithms: a survey. *Computer*, Vol. 27(6), 17-26
- [41] K. De Jong. (1975). An analysis of the behavior of a class of genetic adaptive systems. Technical report, University Microfilms No. 76-9381, Doctoral dissertation, University of Michigan.
- [42] Source: <http://www.stchem.bham.ac.uk/~roy/Research/ga.html>
- [43] Source: http://evolution.berkeley.edu/evolibrary/article/mutations_01
- [44] Source: <http://evolution.berkeley.edu/evosite/evo101/IIIC3aTypes.shtml>
- [45] H. J. Muller, Further studies on the nature and causes of gene mutations, *International Congress of Genetics*.
- [46] Source: http://evolution.berkeley.edu/evolibrary/article/mutations_04
- [47] J. Andre, P. Siarry, and T. Dognon. (2001), An improvement of the standard genetic algorithm fighting premature convergence in continuous optimization, *Advances in engineering software*, vol. 32, no. 1, 49–60
- [48] J. E. Smith and T. C. Fogarty. (1997). Operator and parameter adaptation in genetic algorithms, *Soft computing : a fusion of foundations, methodologies and applications*, vol. 92, no. 2, 81–87.
- [49] S. H. Jung. (2003). Queen-bee evolution for genetic algorithms, *Electronics Letters*, vol. 39, 575–576
- [50] Source: <http://www.nd.com/products/genetic/mutation.htm>
- [51] Sonka, M., & Fitzpatrick, J. M. (2004). *Handbook of medical imaging*. (J. Fitzpatrick, D. L.G.Hill, & J. Calvin R. Maurer, Eds.) Bellingham, Washington: The international society for optical engineering.
- [52] D. B. Fogel. (1994). An Introduction to Simulated Evolutionary Optimization, *IEEE Transactions on Neural Networks*, vol. 5, 3–14
- [53] D.ASIKALA, & Neelaveni, R. (2005). Correlation coefficient measure of multimodal brain image registration using fast Walsh hadamard transform. *Theoretical and applied information technology*, 93-101.
- [54] Woods, R.P., Grafton, S.T., Holmes, C.J., Cherry, S.R. and Mazziotta, J.C. (1994). Automated Image Registration: I. General Methods and Intrasubject, Intramodality Validation, *Journal of Computer Assisted Tomography*, Vol. 12, 153-165,
- [55] Woods, R.P., Grafton, S.T., Watson, J.D.G., Sicotte, N.L. and Mazziotta, J.C. (1994). Automated Image Registration: II. Intersubject Validation of Linear and Nonlinear Models, Vol. 22, 153-65.
- [56] Woods, R.P., Mazziotta, John C and Cherry, S.R. (1994). MRI-PET Registration with Automated Algorithm, *Journal of Computer Assisted Tomography*, Vol.17536- 546.
- [57] Woods, R.P., Cherry, S.R. and Mazziotta, J.C. (1994). Rapid Automated Algorithm for Aligning and Reslicing PET Images, *Journal of Computer Assisted Tomography*, Vol.16, 620-633.

[58] MIVA: <http://ccni.wpi.edu/cwbench/cwbench-tiles.jsp>